J. Min. Metall. Sect. B-Metall. 52 (1) B (2016) 99 - 112

Journal of Mining and Metallurgy, Section B: Metallurgy

PHASE DIAGRAM DETERMINATION AND THERMODYNAMIC MODELING OF THE Cu-Mg-Si SYSTEM

J. Zhao[a,b*], J. Zhou[a], S. Liu[b], Y. Du[b], S. Tang[a], Y. Yang[a]

[a] Shandong Academy of Sciences, Advanced Materials Institute, Shandong Key Laboratory for High Strength Lightweight Metallic Materials (HLM), Shandong Engineering Research Center for Lightweight Automobiles Magnesium Alloy, Jinan, China

[b] Central South University, State Key Laboratory of Powder Metallurgy, Changsha, China

(Received 15 May 2015; accepted 23 December 2015)

Abstract

13 ternary Cu-Mg-Si alloys were prepared by means of the powder metallurgy method. Phase equilibria at 500 and 700 °C of the Cu-Mg-Si system were determined using X-ray diffraction analysis (XRD). The existence of 3 ternary compounds in this system was verified: CuMgSi_Sigma ($Cu_{16}Mg_6Si_7$), Tau (Cu_3Mg_2Si), and Laves ($(Cu_{0.8}Si_{0.2})_2(Mg_{0.88}Cu_{0.12})$). A thermodynamic modeling for the Cu-Mg-Si system was then conducted on the basis of the experimental data obtained in this work and those critically reviewed from the literature. The complex phase relationship between Laves phase and other phases has been successfully modeled in this work. Comparisons between the calculated and the measured phase diagrams show that most of the experimental data can be reproduced by the presently obtained thermodynamic parameters.

Keywords: *Cu-Mg-Si system; XRD analysis; Thermodynamic calculation; Isothermal section; Liquidus projection*

1. Introduction

Al-Cu-Mg-Si system is the basis of a large number of wrought and casting aluminum alloys, e. g. 2XXX, 6XXX series wrought aluminum alloys and 3XX series casting aluminum alloys. The main strengthening mechanism of Al-Cu-Mg-Si alloys depends on the growth control of the precipitates during the heat treatment process [1]. The Cu-Mg-Si system is an important sub-system of the Al-Cu-Mg-Si system. The ternary compounds of Cu-Mg-Si system, such as Cu_3Mg_2Si and $Cu_{16}Mg_6Si_7$, can play as precipitation hardener in Aluminum alloys [2]. A deep understanding of the phase stability in the Cu-Mg-Si system with the change of temperature and composition is essential to promote precipitation hardening of the Al-Cu-Mg-Si alloys. The present work is a continuing effort of our previous attempts [3-6] to establish a thermodynamic database for commercial Al alloys.

Bochvar et al. [7] reviewed almost all the experimental phase diagram and thermodynamic data for the Cu-Mg-Si system in 2006. According to Bochvar et al., most of the experiments available in the literature were performed in the Cu-rich corner and there is a lack of accurate data on phase equilibria of the ternary compounds. There are several thermodynamic descriptions of this system [8-10] based on the literature data. However, these assessments are all limited to the Cu-rich corner and the liquidus surface cannot be reproduced using these thermodynamic parameters. Moreover, some new experimental data were reported in 2014 [11]. Therefore, it is necessary to carry out new measurements and perform a new thermodynamic assessment of the Cu-Mg-Si system.

In the present study, a critical review of the literature data will be made first, and then key alloys will be prepared to determine the phase equilibria at 500 and 700 °C, respectively. Finally, a thermodynamic optimization of the Cu-Mg-Si system will be carried out through the CALPHAD approach.

2. Evaluation of experimental phase diagram data

Many research groups contribute to the experimental measurements on the Cu-Mg-Si system [2,11-24]. Three ternary compounds have been determined: Cu_3Mg_2Si, $Cu_{16}Mg_6Si_7$ and Laves, which directly constitute the characteristic of this system. To facilitate the understanding, all the known phases in Cu-Mg-Si system and their crystallographic data are listed in Table 1.

Portevin and Bonnot [12] claimed the existence of the first ternary compound Cu_3Mg_2Si with the melting

* *Corresponding author: zhaojingrui1008@gmail.com*

DOI:10.2298/JMMB150515009Z

Table 1. *Crystallographic data of solid phases in the Cu-Mg-Si system*

Pearson Symbol/ Space Group/ Prototype	Lattice Parameters (nm)	Atom	WP[a]	X	Y	Z	CN[b]	Ref.
(Cu), solid solution based on Cu								
*cF*4 *Fm*-3*m* Cu	*a*=0.3615	Cu	4*a*	0	0	0	12	[25]
(Mg), solid solution based on Mg								
*hP*2 *P*63/*mmc* Mg	*a*=0.32061 *c*=0.52091	Mg	2*c*	0.3333	0.6667	0.25	12	[26]
(Si), solid solution based on Si								
*cF*8 *Fd*-3*m* C (diamond)	*a*=0.54309	Si	8*a*	0	0	0	4	[27]
hcp_A3, binary Cu-Si phase Cu_7Si								
*hP*2 $P6_3/mmc$ Mg	*a*=0.25547 *c*=0.41758	0.88Cu + 0.12Si	2*c*	0.3333	0.6667	0.25	12	[28]
bcc_A2, binary Cu-Si phase Cu_6Si								
*cI*2 *Im*-3*m* W	*a*=0.2854	-	-	-	-	-	-	[29]
$Cu_{15}Si_4$, binary Cu-Si phase $Cu_{15}Si_4$								
*cI*76 *I*-43*d* $Cu_{15}Si_4$	*a*=0.9694	Cu Si Cu	48*e* 16*c* 12*a*	0.04 0.20833 0.375	0.38 0.20833 0	0.16 0.20833 0.25	13 12 12	[30]
$Cu_{33}Si_7$, binary Cu-Si phase Cu_5Si at higher temperature								
*t***	*a*=0.8815 *c*=0.7903	-	-	-	-	-	-	[29]
$Cu_{56}Si_{11}$, binary Cu-Si phase Cu_5Si at lower temperature								
*cP*20 $P4_132$ βMn	*a*=0.62228	0.83Cu+0.17Si 0.83Cu+0.17Si	12*d* 8*c*	0.125 0.06361	0.20224 0.06361	0.45224 0.06361	-	[31]
Cu_3Si, binary Cu-Si phase Cu_3Si								
*hR** *R*-3*mr*	*a*=0.247 *α*=109.74°	0.75Cu+0.25Si	3*a*	0	0	0	14	[32]
Mg_2Si, binary Mg-Si phase Mg_2Si								
*cF*12 *Fm*-3*m* CaF_2	*a*=0.63447	Mg Si	8*c* 4*a*	0.25 0	0.25 0	0.25 0	10 8	[33]
$CuMg_2$, binary Cu-Mg phase $CuMg_2$								
*oF*48 *Fddd O*2 $CuMg_2$	*a*=0.5275 *b*=0.9044 *c*=1.8328	Mg Cu Mg	16*g* 16*g* 16*f*	0.125 0.125 0.125	0.125 0.125 0.4586	0.0415 0.49819 0.125	15 10 15	[34]
Laves [c], binary Cu-Mg phase Cu_2Mg								
*cF*24 *Fd*-3*mO*2 Cu_2Mg	*a*=0.7021	Cu Mg	16*c* 8*b*	0 0.375	0 0.375	0 0.375	12 16	[35]

Table 1 continued on the next page

CuMgSi_Sigma, ternary compound $Cu_{16}Mg_6Si_7$								
*cF*116 *Fm*-3*m* Mn23Th6	*a*=1.165	Cu Cu Mg Si Si	32*f* 32*f* 24*e* 24*d* 4*a*	0.121 0.334 0.288 0 0	0.121 0.334 0 0.25 0	0.121 0.334 0 0.25 0	13 12 17 12 8	[24]
Tau, ternary compound Cu_3Mg_2Si								
*hP*12 $P6_3/mmc$ Cu_3Mg_2Si (ordered $MgZn_2$)	*a*=0.5001 *c*=0.7872	Cu Mg Si	6*h* 4*f* 2*a*	0.1667 0.3333 0	0.3334 0.6667 0	0.25 0.5625 0	12 16 12	[14]
Laves [c], ternary compound Tau3 with the composition $(Cu_{0.8}Si_{0.2})_2(Mg_{0.88}Cu_{0.12})$								
*cP*24 $P4_132$ (ordered derivative of Cu_2Mg)	*a*=0.69776	0.959Cu+0.041Si 0.882Mg+0.118Cu 0.723Si+0.277Cu	12*d* 8*c* 4*a*	0.125 0.00295 0.375	0.13084 0.00295 0.375	0.38084 0.00295 0.375	12 16 12	[18]

[a] *Wyckoff Positions;* [b] *Coordination Numbers;* [c] *The binary phase Cu_2Mg and ternary phase Tau3 are treated as one phase Laves*

point of 927 °C. They investigated the phase area Mg-$CuMg_2$-Cu_3Mg_2Si-Mg_2Si by means of thermal analysis and micrographic examination. The vertical sections Cu_3Mg_2Si-$CuMg_2$ and Cu_3Mg_2Si-Mg_2Si were found to be "pseudo-binary" with eutectic points at 565 and 857 °C, respectively. Besides, two invariant four-phase equilibria were reported: a ternary transition reaction at 508 °C and 38 wt.% Cu, 0.6 wt.% Si: Liquid+Cu_3Mg_2Si=$CuMg_2$+Mg_2Si, and a ternary eutectic reaction at 479 °C, and 32.5 wt.% Cu, 0.4 wt.% Si: Liquid=Mg+$CuMg_2$+Mg_2Si.

Witte [13,14] investigated the vertical section between the composition $MgCu_2$ and $MgSi_2$ by thermal analysis. His study shows that there is a polymorphic transformation in Cu_3Mg_2Si between 870 and 890 °C: the high temperature form is $MgNi_2$ type (disordered Laves phase with C36 type), whilst the low temperature form is $MgZn_2$ type (ordered Laves phase with C14 type). Witte [13,14] determined the structure of Cu_3Mg_2Si using XRD analysis. He also found the second ternary compound $Cu_{16}Mg_6Si_7$ and investigated its structure.

Komura and Matsunaga [15-18] found the third ternary compound Tau3 near the composition $(Cu_{0.8}Si_{0.2})_2(Mg_{0.88}Cu_{0.12})$. This compound is a new ordered ternary C15 Laves phase. The composition range of the alloys used by Komura and Matsunaga [15-18] is: 25-35 at.% Mg, 10-20 at.% Si, rest Cu. The alloys were annealed at 500 °C for 10 days, and then crushed to small single crystals appropriate for X-ray analysis. The results show that the ternary compound Tau3 exists in solid state at 500 °C. Matsunaga [17,18] determined the homogeneity range of this new compound: 25.5 to 30.0 at.% Mg, 13.5 to 16 at.% Si, rest Cu, but its formation reaction and the highest and lowest temperatures of existence are unknown. In the same investigation [17,18], the homogeneity range of the binary compound Cu_2Mg was established to extend into the ternary system up to 25-33.3 at.% Mg at about 13 at.% Si. These data agree with the results of Klee and Witte [19], who determined that the solubility of Si in Cu_2Mg along the 33.3 at.% Mg section can reach 13.3 at.% using the measurement of magnetic susceptibility.

Using a combination of thermal analysis, optical microscopy, XRD analysis and chemical analysis on 250 alloys, Aschan [20] investigated the phase equilibria of Cu-Mg-Si system in Cu-rich corner and reported a series of three-phase and four-phase invariant equilibria. Bochvar [7] constructed the 450 °C isothermal section of the Cu-Mg-Si system after Aschan [20], and the Tau3 field is corrected according to the data from Matsunaga [15-18] (see Fig. 1).

According to the work of Aschan [20], the ternary compound $Cu_{16}Mg_6Si_7$ is formed from melt by a four-phase peritectic reaction at 826 °C: Cu_2Mg+Cu_3Mg_2Si+liquid=$Cu_{16}Mg_6Si_7$ (826 °C): and the ternary compound Cu_3Mg_2Si is formed from a three-phase peritectic reaction at 930 °C: Cu_2Mg+liquid=Cu_3Mg_2Si (930 °C). It can be seen that both the ternary compounds $Cu_{16}Mg_6Si_7$ and Cu_3Mg_2Si are incongruent melting compounds. This result agrees with the findings of Witte [13,14], therefore we can make a conclusion that there is no pseudo-binary section in this system and the conclusion of Portevin and Bonnot [12] there exist two pseudo-binary sections Cu_3Mg_2Si-$CuMg_2$ and Cu_3Mg_2Si-Mg_2Si is not correct. Fig. 2(a) is the liquidus projection redrawn from Aschan [20]

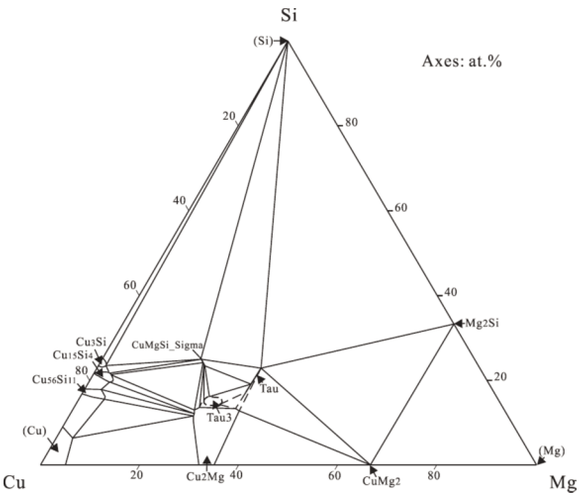

Figure 1. *Cu-Mg-Si isothermal section at 450 °C [7]*

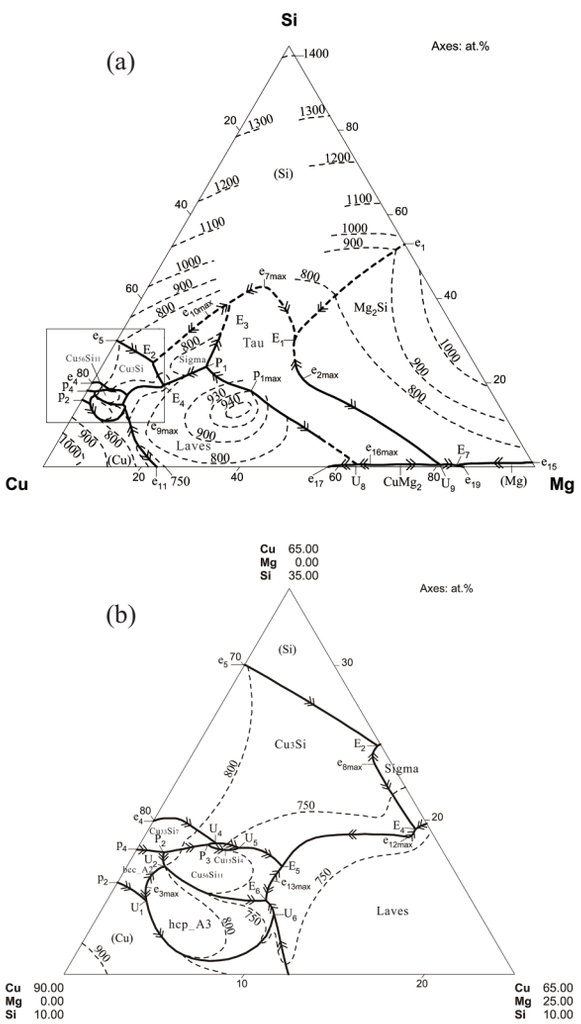

Figure 2. *The projection of the liquidus surface of the Cu-Mg-Si ternary system [7]: (a) in the whole composition range, and (b) in the Cu corner*

replacing mass% for at.% by Bochvar [7]. Fig. 2(b) presents the enlarged view of the copper corner.

Farkas and Birchenall [21] studied the alloy with the composition 56Cu-17Mg-27Si (wt.%) using differential thermal analyses (DTA), XRD, optical microscopy and scanning electron microscopy (SEM) techniques. According to the work of Farkas and Birchenall [21], this alloy is constitute of the ternary eutectic structure, $Cu_{16}Mg_6Si_7$+Mg_2Si+(Si), with the transformation temperature of 770 °C. However, these results are contradict to the work of Aschan [20] and Witte [13,14], who showed the ternary eutectic structure is Cu_3Mg_2Si+Mg_2Si+(Si) for the same composition.

The thermodynamic properties of ternary liquid Cu-Mg-Si alloys along the section x_{Cu}/x_{Si}=7/3 were determined by Ganesan's group [2, 22, 36]. They measured the enthalpies of mixing by isoperibolic calorimetry, and Mg vapor pressures by an isopiestic method. Partial thermodynamic properties of Mg were derived from the vapor pressure data, and the composition dependence of the Mg activities was given for 900 °C [2,22]. They also studied the Cu-Mg-Si phase diagram along the isopleth with x_{Cu}/x_{Si}=7/3 by means of DTA and XRD methods [36].

Arabaci and Yusufoglu [11] determined the thermodynamic properties of ternary Cu-Mg-Si alloys by using thermogravimetric Knudsen effusion method (KEM). The phase boundary compositions in the phase diagram with w_{Cu}/w_{Si} = 20/80 were given in their work [11].

3. Experimental

Due to the high volatility of Mg, it is difficult to prepare samples by the traditional arc-melting method. In the present work, the powder metallurgy method described by He et al. [37] was used. Thirteen Cu-Mg-Si alloys were prepared from pure elemental powders (Cu 99.9 wt.%, Mg 99.99 wt.%, Si 99.9 wt.%). The pure powders were weighed with a high precision balance with an accuracy of 0.0001 g, and then the powders were blended in a mechanical mixer. After mixing, the powders were pressed into green compacts with a powder metallurgy die of 10 mm diameter. After that, the green compacts were put into iron tubes. These iron tubes were sealed by arc melting in a vacuum arc furnace (WKDHL-I, Opto-electronics Co. Ltd., Beijing) in a high-purity Ar (99.9999 %) atmosphere. All the iron tubes were put in a muffle furnace at 800 °C for 2 hours. Then some of the alloys (1#-9#) were annealed in a tube-type furnace at 500 °C for 60 days, and the others (10#-13#) were annealed in the muffle furnace at 700 °C for 50 days. After annealing, the alloys were quenched in cold water. Finally, all the alloys were pulverized in an agate mortar and analyzed using

XRD (Rigaku D/max2550VB, Japan). The phases present in the alloys were identified using MDI (Materials Data Inc.) Jade 5.0 software and the ICDD-PDF database.

4. Thermodynamic model

In the present modeling, the Gibbs energy functions of pure elements Cu, Mg and Si were taken from the SGTE (Scientific Group Thermodata Europe) compilation [38]. The thermodynamic parameters in the Cu-Mg, Cu-Si and Mg-Si binary systems were taken from references [39], [40] and [41], respectively. The calculated binary phase diagrams are presented in Figs. 3(a)-(c).

The phases in the Cu-Mg-Si system to be optimized in this work are as follows: liquid; binary phases, $Cu_{15}Si_4$ and $Cu_{56}Si_{11}$; three ternary compounds, CuMgSi_Sigma ($Cu_{16}Mg_6Si_7$), Tau (Cu_3Mg_2Si), and Laves (Tau3). Different models were employed to describe the above mentioned phases.

4.1 Solution phases

The solution phases, i.e., liquid, fcc_A1 (Cu), hcp_A3 (Mg), and diamond_A4 (Si) were described with the substitutional solution model.

The molar Gibbs energy of phase ϕ (ϕ representing the aforementioned solution phases) is expressed as below:

$$G_m^{\phi} = \sum_{i=Cu,\mathrm{Mg,Si}} x_i \, {}^{0}G_i^{\phi} + RT \sum_{i=Cu,\mathrm{Mg,Si}} x_i \ln(x_i) + {}^{ex}G^{\phi} \qquad (1)$$

where R is the gas constant, T is the temperature in K, x_i is the mole fraction of component i (i=Cu, Mg and Si), ${}^{0}G_i^{\phi}$ is the molar Gibbs energy of pure element i at 25 °C and 1 bar, in its standard element reference (SER) state [38], and ${}^{ex}G^{\phi}$ is the excess Gibbs energy, expressed by a Redlich-Kister polynomial [42]:

$$\begin{aligned} {}^{ex}G^{\phi} = {} & x_{Cu}x_{Mg}\sum_{j=0,1\ldots}^{N} {}^{(j)}L_{Cu,Mg}^{\phi}(x_{Cu}-x_{Mg})^{j} + \\ & + x_{Cu}x_{Si}\sum_{j=0,1\ldots}^{N} {}^{(j)}L_{Cu,\mathrm{Si}}^{\phi}(x_{Cu}-x_{Si})^{j} + \\ & + x_{Mg}x_{Si}\sum_{j=0,1\ldots}^{N} {}^{(j)}L_{\mathrm{Mg,Si}}^{\phi}(x_{Mg}-x_{Si})^{j} + \\ & + x_{Cu}x_{Mg}x_{Si}(x_{Cu}\,{}^{(0)}L_{Cu,Mg,Si}^{\phi} + \\ & + x_{Mg}\,{}^{(1)}L_{Cu,Mg,Si}^{\phi} + x_{Si}\,{}^{(2)}L_{Cu,Mg,Si}^{\phi}) \end{aligned} \qquad (2)$$

where ${}^{(j)}L_{Cu,Mg}^{\phi}$, ${}^{(j)}L_{Cu,Si}^{\phi}$ and ${}^{(j)}L_{Mg,Si}^{\phi}$ are the interaction parameters of ϕ phase from the binary systems Cu-Mg, Cu-Si and Mg-Si. ${}^{(k)}L_{Cu,Mg,Si}^{\phi}$ denotes the ternary interaction parameter among Cu, Mg and Si, which is expressed as:

$${}^{(k)}L_{Cu,Mg,Si}^{\phi} = A + BT \qquad (3)$$

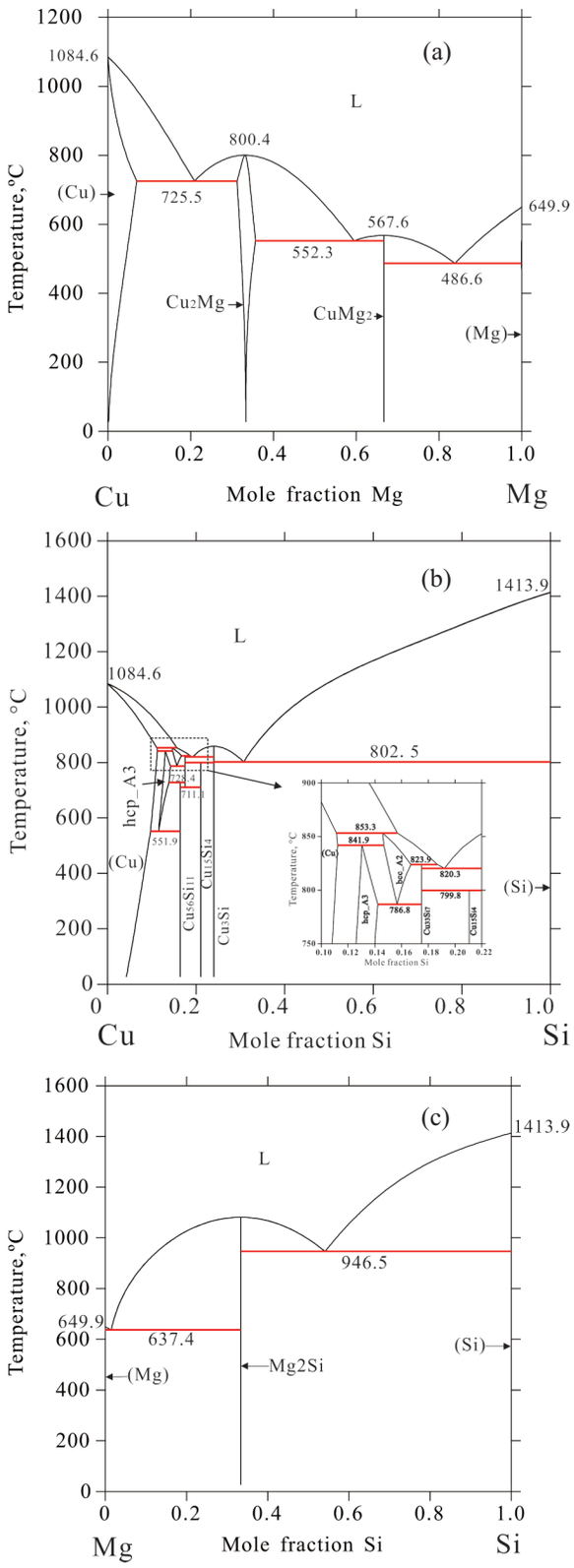

Figure 3. *Calculated phase diagrams of (a) Cu-Mg, (b) Cu-Si and (c) Mg-Si binary systems according to [39], [40] and [41], respectively*

where A and B are the parameters to be optimized. In this work, only the ternary interaction parameters for liquid were optimized.

4.2 Binary intermetallic phases

Both the binary phases $Cu_{15}Si_4$ and $Cu_{56}Si_{11}$ exhibit some solubility for Mg [20]. They were described with the sublattice model (**Cu**, $Mg)_{0.789474}Si_{0.210526}$ and (**Cu**, $Mg)_{0.835821}Si_{0.164179}$, respectively, with Mg atoms dissolving in the first sublattice only. The boldfaces mean normal atoms (i.e., major species) in the sublattice. The Gibbs energy of the phase (**Cu**, $Mg)_mSi_n$ per mole formula is described by the Compound-Energy Formalism, which is expressed as:

$$\begin{aligned} G^{(Cu,Mg)_mSi_n} &= y'_{Cu}G^{(Cu,Mg)_mSi_n}_{Cu:Si} + y'_{Mg}G^{(Cu,Mg)_mSi_n}_{Mg:Si} + \\ &+ mRT(y'_{Cu}\ln y'_{Cu} + y'_{Mg}\ln y'_{Mg}) + \\ &+ y'_{Cu}y'_{Mg}[\sum_{j=0,1...}^{N} {}^{j}L^{(Cu,Mg)_mSi_n}_{Cu,Mg:Si}(y'_{Cu}-y'_{Mg})^j] \end{aligned} \quad (4)$$

where y'_{Cu} and y'_{Mg} are the site fractions of Cu and Mg in the first sublattice. The parameters denoted as $G^{(Cu,Mg)_mSi_n}_{Cu:Si}$ and $G^{(Cu,Mg)_mSi_n}_{Mg:Si}$ are the Gibbs energy of the formation of the so-called "end-members". The parameter ${}^{j}L^{(Cu,Mg)_mSi_n}_{Cu,Mg:Si}$ represents the interactions of Cu and Mg within the first sublattice.

4.3 Ternary phases

The ternary compounds CuMgSi_Sigma phase ($Cu_{16}Mg_6Si_7$) and Tau phase (Cu_3Mg_2Si) were described with the stoichiometric model. The Gibbs energy of CuMgSi_Sigma phase ($Cu_{16}Mg_6Si_7$) is expressed as follows:

$$\begin{aligned} G^{CuMgSi\_Sigma} &= 16\times G^{0,fcc}_{Cu} + 6\times G^{0,hcp}_{Mg} + 7\times G^{0,dia}_{Si} + \\ &+ a + bT \end{aligned} \quad (5)$$

where $a+bT$ is the formation energy of one mole formula compound. a and b are parameters to be optimized in this work. An analogous equation can be written for the Gibbs energy of Tau phase and its formula is changed into $Cu_{2.74}Mg_2Si_{1.26}$ according to the experimental results of this work.

The third compound Tau3 phase, $(Cu_{0.8}Si_{0.2})_2(Mg_{0.88}Cu_{0.12})$, is an ordered laves_C15 structure phase, which is formed by the extension of the binary Cu_2Mg phase to the Cu-Mg-Si ternary phase region, but the highest and lowest temperatures for its presence as well as its phase relationship with other phases are still unknown. According to the study of Klee and Witte [19], the solubility of Si in Cu_2Mg can be up to 13.3 at.% along the section of 33.3 at.% Mg. In the present work, the third ternary compound Tau3 and the binary compound Cu_2Mg were modeled as one phase Laves: (**Cu**, Mg, $Si)_2$(Cu, **Mg**, Si), which is consistent with the modeling of laves_C15 phase in other ternary systems such as Al-Cu-Mg and Cu-Mg-Ni [43]. There are 9 ideal (or hypothetical) compounds and 18 interaction parameters in this model. The Gibbs energy of Laves phase per mole formula is expressed as follows:

$$\begin{aligned} G^{Laves} - H^{SER} &= y'_{Cu}\,y''_{Cu}\,{}^{0}G^{Laves}_{Cu:Cu} + y'_{Mg}\,y''_{Mg}\,{}^{0}G^{Laves}_{Mg:Mg} + \\ &+ y'_{Si}\,y''_{Si}\,{}^{0}G^{Laves}_{Si:Si} + y'_{Cu}\,y''_{Mg}\,{}^{0}G^{Laves}_{Cu:Mg} + \\ &+ y'_{Mg}\,y''_{Cu}\,{}^{0}G^{Laves}_{Mg:Cu} + y'_{Cu}\,y''_{Si}\,{}^{0}G^{Laves}_{Cu:Si} + \\ &+ y'_{Si}\,y''_{Cu}\,{}^{0}G^{Laves}_{Si:Cu} + y'_{Si}\,y''_{Mg}\,{}^{0}G^{Laves}_{Si:Mg} + \\ &+ y'_{Mg}\,y''_{Si}\,{}^{0}G^{Laves}_{Mg:Si} + 2RT(y'_{Cu}\ln y'_{Cu} + \\ &+ y'_{Mg}\ln y'_{Mg} + y'_{Si}\ln y'_{Si}) + \\ &+ RT(y''_{Cu}\ln y''_{Cu} + y''_{Mg}\ln y''_{Mg} + \\ &+ y''_{Si}\ln y''_{Si}) + y'_{Cu}\,y'_{Si}(y''_{Cu}\,L^{Laves}_{Cu,Si:Cu} + \\ &+ y''_{Mg}\,L^{Laves}_{Cu,Si:Mg} + y''_{Si}\,L^{Laves}_{Cu,Si:Si}) + \\ &+ y'_{Cu}\,y'_{Mg}(y''_{Cu}\,L^{Laves}_{Cu,Mg:Cu} + y''_{Mg}\,L^{Laves}_{Cu,Mg:Mg} + \\ &+ y''_{Si}\,L^{Laves}_{Cu,Mg:Si}) + y'_{Mg}\,y'_{Si}(y''_{Cu}\,L^{Laves}_{Mg,Si:Cu} + \\ &+ y''_{Mg}\,L^{Laves}_{Mg,Si:Mg} + y''_{Si}\,L^{Laves}_{Mg,Si:Si}) + y''_{Cu}\,y''_{Si} \\ &(y'_{Cu}\,L^{Laves}_{Cu:Cu,Si} + y'_{Mg}\,L^{Laves}_{Mg:Cu,Si} + y'_{Si}\,L^{Laves}_{Si:Cu,Si}) \\ &+ y''_{Cu}\,y''_{Mg}(y'_{Cu}\,L^{Laves}_{Cu:Cu,Mg} + y'_{Mg}\,L^{Laves}_{Mg:Cu,Mg} + \\ &+ y'_{Si}\,L^{Laves}_{Si:Cu,Mg}) + y''_{Mg}\,y''_{Si}(y'_{Cu}\,L^{Laves}_{Cu:Mg,Si} + \\ &+ y'_{Mg}\,L^{Laves}_{Mg:Mg,Si} + y'_{Si}\,L^{Laves}_{Si:Mg,Si}) \end{aligned} \quad (6)$$

where y'_{Cu}, y'_{Mg} *and* y'_{Si} are the mole fractions of Cu, Mg and Si in the first sublattice, while y''_{Cu}, y''_{Mg} *and* y''_{Si} are the mole fractions of Cu, Mg and Si in the second sublattice, respectively.

4.4 Optimization procedure

The evaluation of the model parameters is attained by recurrent runs of the PARROT module in the Thermo-Calc program [44], which works by minimizing the sum of squares of the differences between experimental values and computed ones. The step-by-step optimization procedure described by Du et al. [45] in detail was utilized in the present assessment. First, the thermodynamic parameters of the liquid phase were obtained preliminarily using the data of the thermodynamic properties of the liquid phase. Next, the thermodynamic parameters of the ternary compounds were optimized using the data of the phase equilibria at 450, 500 and 700 °C. Then, the ternary interactive parameters of the binary Cu-Si compounds were introduced. Finally, with a comprehensive consideration of the data of the liquid projection, isothermal sections, vertical sections, and the thermodynamic property data of the liquid phase, the thermodynamic parameters of the liquid phase, ternary phases and the binary Cu-Si compounds were

optimized, to make sure that the thermodynamic parameters obtained in this work can reproduce the experimental data of the Cu-Mg-Si system.

5. Results and discussions

5.1 Experimental results

The XRD results of the alloys in this work are listed in Table 2. The existence of the three ternary compounds was confirmed and partial phase equilibrium relationships of them were identified. The experimental results show that Laves, Tau and CuMgSi_Sigma are stable at both 500 and 700 °C. In the investigated samples, the following three-phase regions: Laves + Tau + CuMgSi_Sigma, Tau + Mg_2Si + (Si), Tau + Laves + $CuMg_2$, and Mg_2Si + $CuMg_2$ + (Mg), and the two-phase region: Laves + (Cu) were identified at 500 °C; the two-phase regions: Laves + (Cu), Laves + Tau, and CuMgSi_Sigma + Cu_3Si were identified at 700 °C.

Table 2. *Cu-Mg-Si alloy compositions and phases coexisting upon equilibration at 500 °C and 700 °C according to the XRD results*

Alloy No.	Composition (at. %)			Ann. temp. (°C)	Coexisting phases
	Cu	Mg	Si		
1	10	40	50	500	Mg_2Si+(Si)+ Tau
2	67	20	13	500	Laves+(Cu)
3	50	37	13	500	Tau + Laves+$CuMg_2$
4	15	72	13	500	Mg_2Si+$CuMg_2$+(Mg)
5	5	82	13	500	Mg_2Si+$CuMg_2$+(Mg)
6	79	12	9	500	Laves+(Cu)
7	50	33.3	16.7	500	Tau + Laves+ CuMgSi_Sigma
8	45.7	33.3	21	500	Tau + Laves+ CuMgSi_Sigma
9	75	20	5	500	Laves+(Cu)
10	67	20	13	700	(Cu)+ Laves
11	79	12	9	700	(Cu)+ Laves
12	45.7	33.3	21	700	Laves+ Tau
13	55.2	20.7	24.1	700	CuMgSi_Sigma +Cu_3Si

5.2 Thermodynamic calculation results

The assessed thermodynamic parameters for the Cu-Mg-Si system are listed in Table 3.

Fig. 4 shows the calculated isothermal section at 450 °C with the comparison of the experimental data from literature [20]. Fig. 4(a) is the isothermal section in the whole composition range, and Fig. 4(b) the area in the Cu-rich corner. It can be seen that the calculated

Table 3. *Thermodynamic models and parameters of the Cu-Mg-Si ternary system (Parameters are valid in temperature interval 298.15 < T < 2500 K)*

Phase: L; Model: $(Cu,Mg,Si)_1$

$${}^{ex}G^{L}_{Cu,Mg,Si} = x_{Cu}\cdot x_{Mg}\cdot x_{Si}[(-27023.6+32.0757\cdot T)x_{Cu} + (-20909.7+29.7609\cdot T)x_{Mg} + (-287407-2.87573\cdot T)x_{Si}]$$

Phase: CuMgSi_Sigma; Model: $Cu_{16}Mg_6Si_7$

$${}^{0}G^{CuMgSi\_Sigma}_{Cu:Mg:Si} - 16\,{}^{0}G^{fcc\_A1}_{Cu} - 6\,{}^{0}G^{hcp\_A3}_{Mg} - 7\,{}^{0}G^{diamond\_A4}_{Si} = -506236+20.0884\cdot T$$

Phase:Tau; Model: $Cu_{2.74}Mg_2Si_{1.26}$

$${}^{0}G^{Tau}_{Cu:Mg:Si} - 2.74\,{}^{0}G^{fcc\_A1}_{Cu} - 2\,{}^{0}G^{hcp\_A3}_{Mg} - 1.26\,{}^{0}G^{diamond\_A4}_{Si} = -129354+8.43518\cdot T$$

Phase: Laves; Model: $(Cu, Mg, Si)_2(Cu, Mg, Si)_1$

$${}^{0}G^{Laves}_{Cu:Cu} - 3\,{}^{0}G^{fcc\_A1}_{Cu} = 15000$$

$${}^{0}G^{Laves}_{Mg:Cu} - 2\,{}^{0}G^{hcp\_A3}_{Mg} - {}^{0}G^{fcc\_A1}_{Cu} = 104971-16.4645\cdot T$$

$${}^{0}G^{Laves}_{Si:Cu} - 2\,{}^{0}G^{diamond\_A4}_{Si} - {}^{0}G^{fcc\_A1}_{Cu} = 90000$$

$${}^{0}G^{Laves}_{Cu:Mg} = -54690.99+364.73085\cdot T - 69.276417\cdot T\cdot\ln(T) - 5.19246\cdot 10^{-4}\cdot T^2 + 143502\cdot T^{-1} - 5.65953\cdot 10^{-6}\cdot T^3$$

$${}^{0}G^{Laves}_{Mg:Mg} - 3\,{}^{0}G^{hcp\_A3}_{Mg} = 15000$$

$${}^{0}G^{Laves}_{Si:Mg} - 2\,{}^{0}G^{diamond\_A4}_{Si} - {}^{0}G^{hcp\_A3}_{Mg} = 90000$$

$${}^{0}G^{Laves}_{Cu:Si} - 2\,{}^{0}G^{fcc\_A1}_{Cu} - {}^{0}G^{diamond\_A4}_{Si} = 90000$$

$${}^{0}G^{Laves}_{Mg:Si} - 2\,{}^{0}G^{hcp\_A3}_{Mg} - {}^{0}G^{diamond\_A4}_{Si} = 90000$$

$${}^{0}G^{Laves}_{Si:Si} - 3\,{}^{0}G^{diamond\_A4}_{Si} = 90000$$

$${}^{0}G^{Laves}_{Cu,Mg:Cu} = 13011.35$$

$${}^{0}G^{Laves}_{Cu:Cu,Mg} = 6599.45$$

$${}^{0}G^{Laves}_{Mg:Cu,Mg} = 6599.45$$

$${}^{0}G^{Laves}_{Cu,Mg:Mg} = 13011.35$$

$${}^{0}G^{Laves}_{Mg,Si:Mg} = 15000$$

$${}^{0}G^{Laves}_{Mg,Si:Si} = 15000$$

$${}^{0}G^{Laves}_{Cu,Si:Mg} = -291567+110\cdot T$$

$${}^{0}G^{Laves}_{Cu:Mg,Si} = -234365+16\cdot T$$

Phase: $Cu_{15}Si_4$; Model: $(Cu, Mg)_{0.789474}Si_{0.210526}$

$${}^{0}G^{Cu_{15}Si_4}_{Cu:Si} - 0.789474\,{}^{0}G^{fcc\_A1}_{Cu} - 0.210526\,{}^{0}G^{diamond\_A4}_{Si} = 1240.9639 - 6.7191165\cdot T$$

$${}^{0}G^{Cu_{15}Si_4}_{Mg:Si} - 0.789474\,{}^{0}G^{hcp\_A3}_{Mg} - 0.210526\,{}^{0}G^{diamond\_A4}_{Si} = 5000$$

$${}^{0}G^{Cu_{15}Si_4}_{Cu,Mg:Si} = -40000+25\cdot T$$

Phase: $Cu_{56}Si_{11}$; Model: $(Cu, Mg)_{0.835821}Si_{0.164179}$

$${}^{0}G^{Cu_{56}Si_{11}}_{Cu:Si} - 0.835821\,{}^{0}G^{fcc\_A1}_{Cu} - 0.164179\,{}^{0}G^{diamond\_A4}_{Si} = 1046.4873 - 5.8746832\cdot T$$

$${}^{0}G^{Cu_{56}Si_{11}}_{Mg:Si} - 0.835821\,{}^{0}G^{hcp\_A3}_{Mg} - 0.164179\,{}^{0}G^{diamond\_A4}_{Si} = 5000$$

$${}^{0}G^{Cu_{56}Si_{11}}_{Cu,Mg:Si} = -37000+3\cdot T$$

results agree with the literature [20]. Fig. 5 and Fig. 6 show the calculated isothermal sections of Cu-Mg-Si system at 500 and 700 °C, respectively. The composition points of the alloys used in the present experimental work are also shown for comparison. Combined with Table 2, it can be seen that the calculated results agree well with the experimental results. Fig. 7 shows the calculated vertical section along Cu_7Si_3-Mg compared with the literature data [36]. The calculated results agree with most of the literature data except for some discrepancies, i.e., the calculated liquidus temperature of Mg_2Si is higher than the literature value, and the calculated temperature of the four-phase equilibrium, L+Tau=Mg_2Si+$CuMg_2$ (U10), is higher than the literature data [36]. Fig. 8 shows the calculated mixing enthalpy of ternary liquid Cu-Mg-Si alloys with x_{Cu}/x_{Si} = 7/3 compared with the experimental data from Ganesan et al. [2]. It can be seen that in the

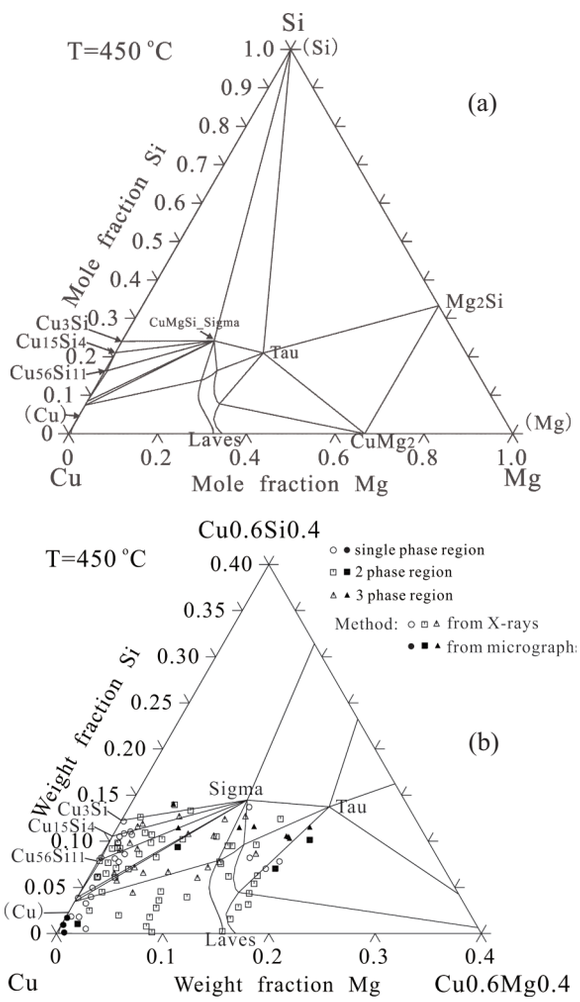

Figure 4. *Calculated isothermal section at 450 °C of the Cu-Mg-Si system: (a) in full composition range, and (b) in Cu corner compared with the experimental data from [20]*

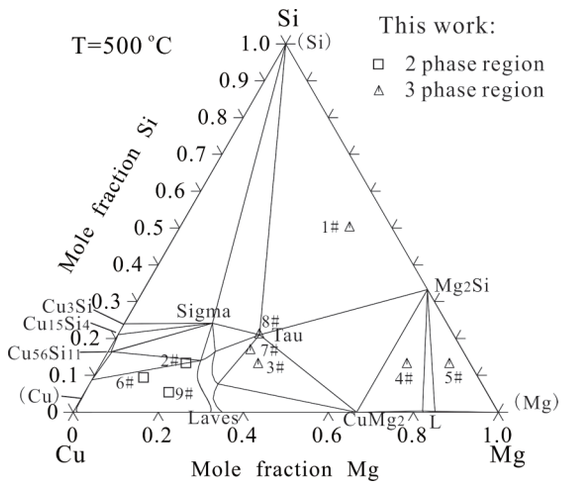

Figure 5. *Calculated isothermal section at 500 °C of the Cu-Mg-Si system with the composition points of the alloys used in the present work*

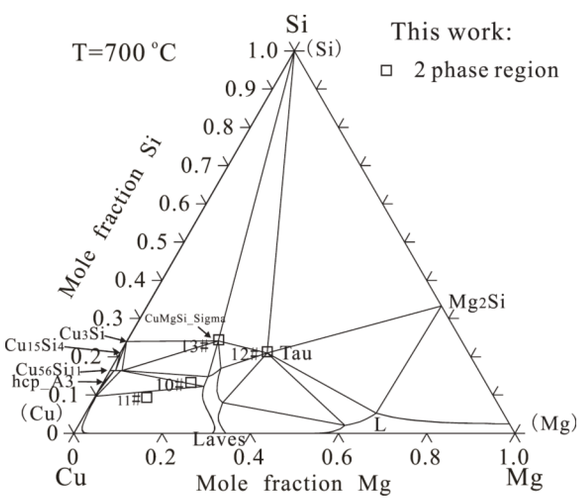

Figure 6. *Calculated isothermal section at 700 °C of the Cu-Mg-Si system with the composition points of the alloys used in the present work*

Mg-rich side, the calculated results agree well with the experimental data, but near the Cu-Si side there is a discrepancy between them. This discrepancy is apparently caused by the thermodynamic parameters of the binary Cu-Si system, which is not consistent with the experimental data from Ganesan et al. [2]. Fig. 9 shows the calculated activities of Mg in liquid phase at 900 °C along the isopleth x_{Cu}/x_{Si} =7/3. The calculated results agree well with the literature data [2].

Fig. 10 shows the calculated vertical section of w_{Cu}/w_{Si}=20/80 in the Cu-Mg-Si system. The calculated results are in good agreement with the phase boundary compositions obtained from Arabaci and Yusufoglu's work [11].

Fig. 11(a) and (b) show the calculated liquidus

projection of Cu-Mg-Si system using thermodynamic parameters obtained in the present work. Compared with the liquidus projection constructed from the literature data (see Fig. 2(a) and (b)), the phase relationships and the main geometric features of Fig. 11 and Fig. 2 are consistent with each other. Table 4 lists the temperatures of the invariant equilibria calculated using the presently obtained thermodynamic parameters compared with those from literature. It can be seen from Table 4 that the ternary compound Tau is formed from a three-phase peritectic reaction : L+Laves=Tau(p1,max), while the CuMgSi_Sigma phase is formed from a three-phase eutectic reaction: L = Laves + CuMgSi_Sigma (e2,max). Both the phases Tau and CuMgSi_Sigma are incongruent melting compounds, so there are no pseudo-binary vertical sections in this system. This conclusion is consistent with the study of Aschan [20] and Witte [13, 14]. Fig. 12 shows the Scheil reaction scheme developed based on the present calculation.

Compared with the invariant reaction temperatures from literature, some of the temperatures calculated in this work have some differences (greater than 20 °C). There are three main causes for this: 1. No ternary interaction parameters were introduced for most of the binary phases; 2. The optimization was conducted from the overall point of view of the phase relationships and some parts can not be well satisfied; 3. There exist deviations between the experimental data from literature and more work is needed for the verification.

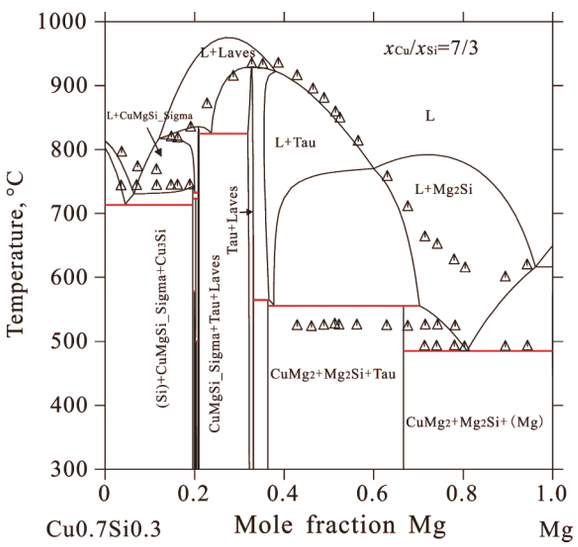

Figure 7. *Calculated Cu_7Si_3-Mg vertical section compared with experimental data from [36]*

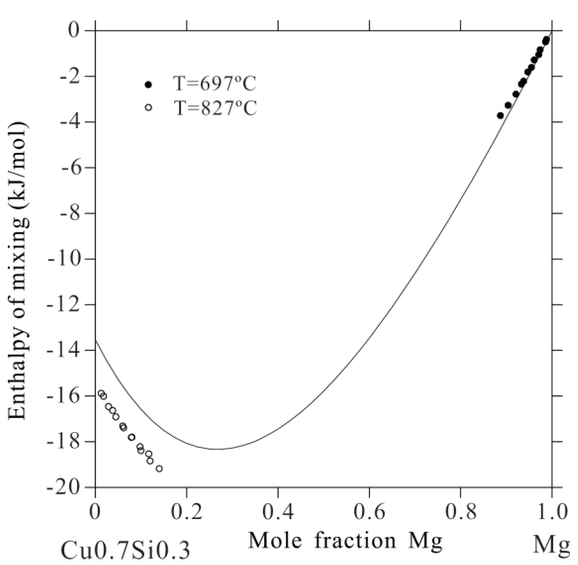

Figure 8. *Calculated enthalpy of mixing for ternary liquid Cu-Mg-Si alloys with xCu/xSi = 7/3 (the referring state is liquid) compared with the experimental data from [2]*

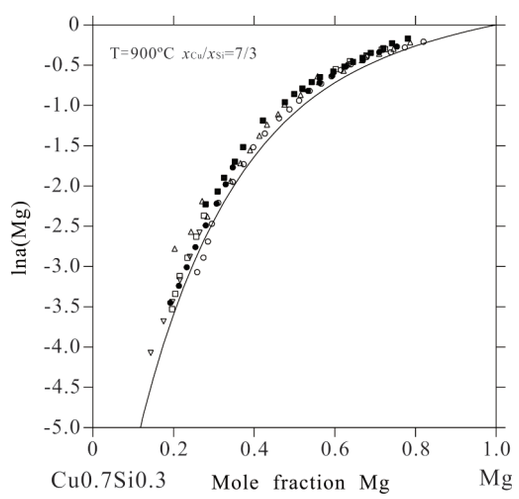

Figure 9. *Calculated natural logarithm of the magnesium activity for liquid Cu-Mg-Si alloys along the isopleth with xCu/xSi = 7/3 at 900 °C, compared with the experimental data from [2]*

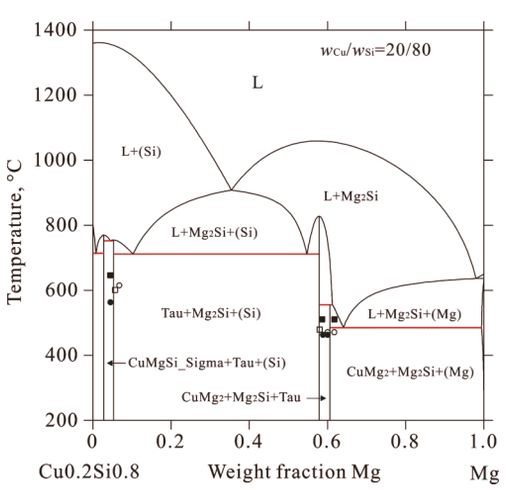

Figure 10. *Calculated wCu/wSi=20/80 isopleth compared with the literature data (points denote the phase boundary compositions obtained from [11])*

Table 4. *Calculated invariant equilibria compared with the literature data*

Symbol	Invariant Reaction	Temperature/°C (literature data)	Temperature/°C (calculated in this work)	Difference between the calculation and the literature data
p1,max	L+Laves=Tau	930 [20] 927(melting point) [12]	930	0
e2,max	L=Laves+CuMgSi_Sigma		835.81	
U1	(Cu)+bcc_A2=L+hcp_A3	824 [20]	839.72	15.72
U2	L+Laves=Tau+CuMgSi_Sigma	826 [20]	825.1	-0.9
P1	$L+Cu_{33}Si_7+Cu_3Si=Cu_{15}Si_4$	763 [20]	804.9	41.9
U3	$L+bcc\_A2=Cu_{56}Si_{11}+hcp\_A3$	800 [20]	796.9	-3.1
U4	$L+bcc\_A2=Cu_{56}Si_{11}+Cu_{33}Si_7$	806 [20]	796.69	-9.31
U5	$L+hcp\_A3=(Cu)+Cu_{56}Si_{11}$		787.86	
U6	$L+Cu_{33}Si_7=Cu_{56}Si_{11}+Cu_{15}Si_4$	772 [20]	784.72	12.72
U7	$L+Cu_{15}Si_4=Cu_3Si+Cu_{56}Si_{11}$	745 [20]	775.28	30.28
E1	$L=(Cu)+Cu_{56}Si_{11}+Laves$		759.7	
E2	L=CuMgSi_Sigma+Tau+(Si)		752.33	
U8	$L+CuMgSi\_Sigma=Laves+Cu_3Si$	723 [20]	732.44	9.44
E3	$L=Laves+Cu_3Si+Cu_{56}Si_{11}$	701 [20]	732.09	31.09
E4	$L=CuMgSi\_Sigma+Cu_3Si+(Si)$	739 [20]	713.46	-25.54
		742 [23]		-28.54
E5	$L=Tau+Mg_2Si+(Si)$	760 [14]	711.17	-48.83
U9	$L+Laves=CuMg_2+Tau$		564.82	
U10	$L+Tau=Mg_2Si+CuMg_2$	508 [12]	555.44	47.44
		524 [23]		31.44
E6	$L=(Mg)+Mg_2Si+CuMg_2$	479 [12]	485.34	6.34
		491.5 [23]		-6.16

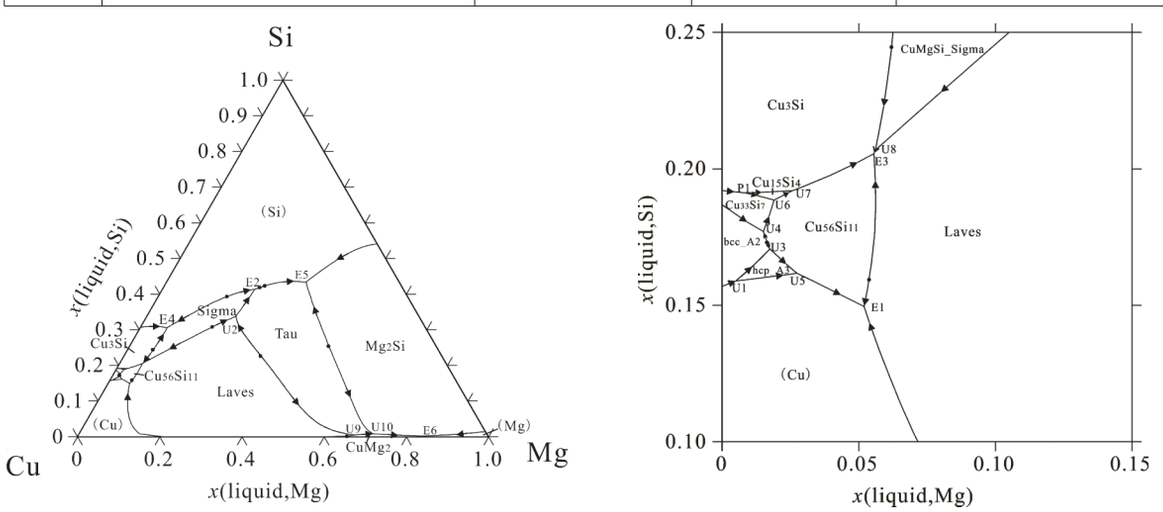

Figure 11. *Calculated liquidus projection of the Cu-Mg-Si ternary system using the parameters of the present work: (a) in the whole composition range, and (b) in the Cu-rich corner*

Through the comparisons of the calculated isothermal sections, vertical sections, thermodynamic property diagrams and liquidus projection with the experimental ones (Figs. 4-11), one can see that the thermodynamic parameters obtained in the present work can reasonably describe the Cu-Mg-Si system.

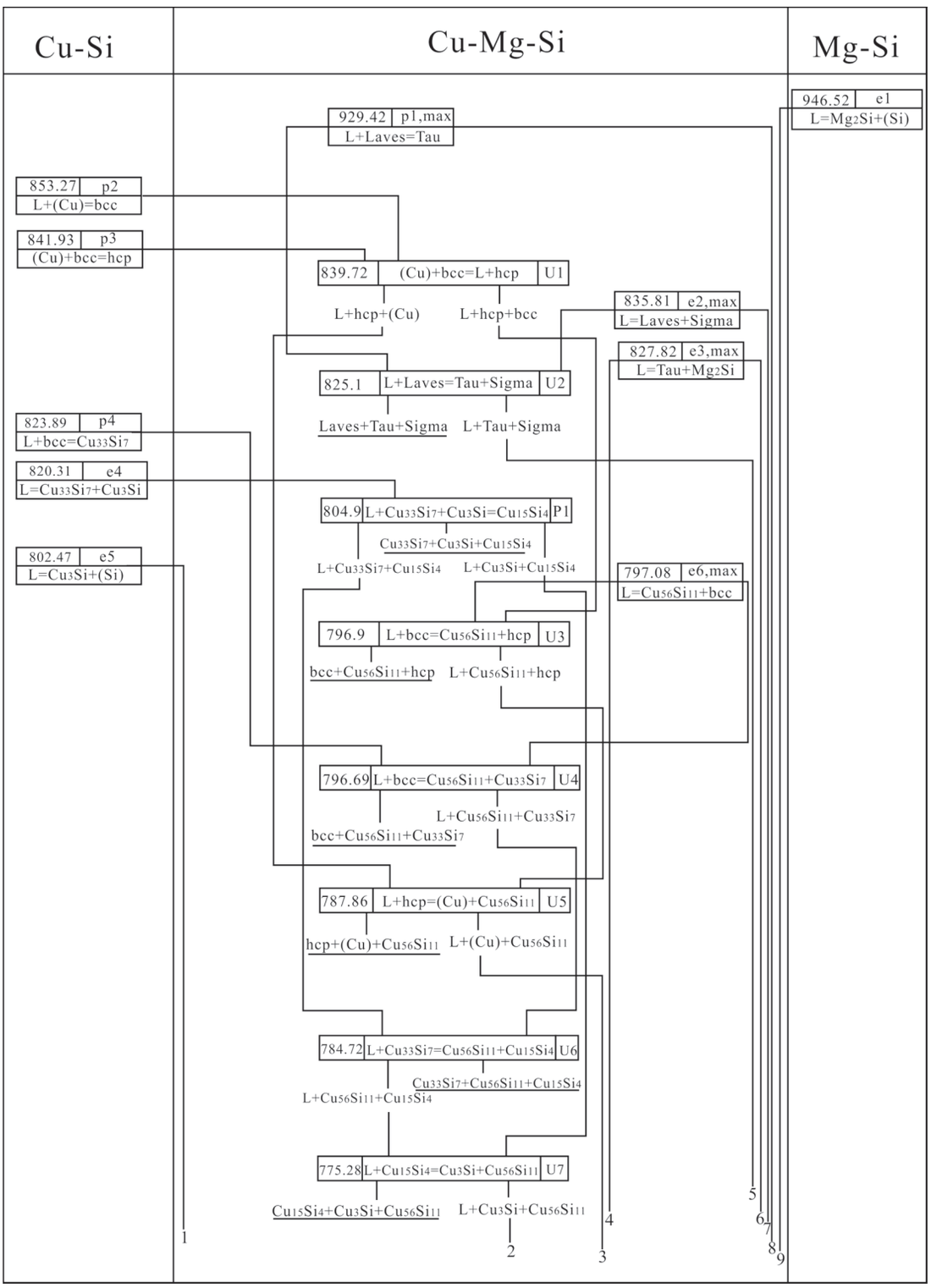

Figure 12. *Scheil reaction scheme of Cu-Mg-Si system obtained from this work: (a) part 1*

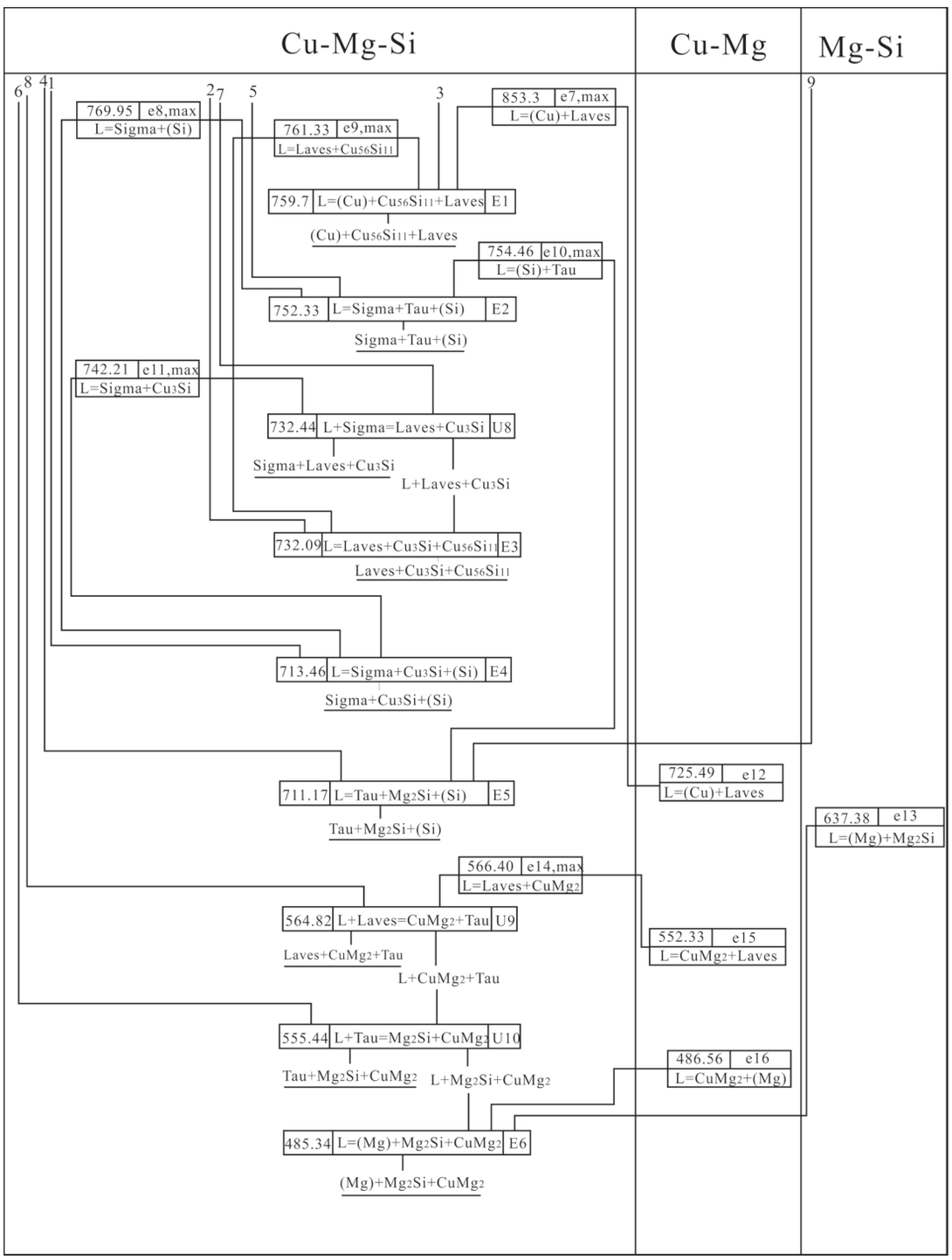

Figure 12. *Scheil reaction scheme of Cu-Mg-Si system obtained from this work: (b) part 2. Note: Sigma denotes CuMgSi_Sigma phase*

6. Conclusions

13 Cu-Mg-Si alloys were prepared. Through the XRD analysis, the isothermal sections of Cu-Mg-Si system at 500 and 700 ºC were determined. The results confirmed the existence of the three ternary compounds CuMgSi_Sigma ($Cu_{16}Mg_6Si_7$), Tau (Cu_3Mg_2Si) and Laves phase.

A critical review was conducted to the literature data of the Cu-Mg-Si system. On the basis of the

phase diagram and thermodynamic data from literature, combined with the experimental results of the present work, a thermodynamic optimization was conducted to the Cu-Mg-Si system. The comprehensive comparisons with the experimental data show that the thermodynamic parameters obtained in this work can describe most of the experimental data.

The liquidus projection of the Cu-Mg-Si system was calculated and the phase relationships are consistent with the ones from literature.

Acknowledgements

The financial support from the National Basic Research Program of China (Grant No. 2014CB644002), the National Natural Science Foundation of China (Grant No. 51531009), the Youth Foundation of Shandong Academy of Sciences (Grant No. 2014QN024) and Thermo-Calc Software AB under the Aluminum Alloy Database Project is greatly acknowledged.

References

[1] S. Zafar, N. Ikram, M.A. Shaikh, K.A. Shoaib, J. Mater. Sci., 25 (5) (1990) 2595-2597.

[2] V. Ganesan, H. Feufel, F. Sommer, H. Ipser, Metall. Mater. Trans. B, 29 (4) (1998) 807-813.

[3] Y. Du, J. Zhao, C. Zhang, H. Chen, L. Zhang, J. Min. Metall. Sect. B-Metall., 43 (1) (2007) 39-56.

[4] J. Zhao, L. Zhang, Y. Du, H. Xu, J. Liang, B. Huang, Metall. Mater. Trans. A, 40 (8) (2009) 1811-1825.

[5] J. Li, T. Liu, W. Chen, S. Wang, L. Zhang, Y. Du, H. Xu, J. Min. Metall. Sect. B-Metall., 50 (2) (2014) 93-99.

[6] B. Hu, Y. Du, J.-J. Yuan, Z.-F. Liu, Q.-P. Wang, J. Min. Metall. Sect. B-Metall. 51 (2) (2015) 125-132.

[7] N. Bochvar, E. Lysova, L. Rokhlin, in Light metal ternary systems: phase diagrams, crystallographic and thermodynamic data (G. Effenberg, S. Ilyenko), Materials Science International Services GmbH, Stuttgart, 2006, p.224-237.

[8] T. Büehler, in COST 507-Thermochemical database for light metal alloys (I. Ansara, A.T. Dinsdale, M.H. Rand), Office for Official Publications of the European Communities, Luxembourg, 1998, p.360-362.

[9] X. Yan, Thermodynamic and solidification modeling coupled with experimental investigation of the multicomponent aluminum alloys, University of Wisconsin-Madison, 2001.

[10] J. Miettinen, G. Vassilev, Cryst. Res. Technol., 46 (11) (2011) 1122-1130.

[11] A. Arabaci, I. Yusufoglu, Metall. Mater. Trans. A, 45 (4) (2014) 1803-1812.

[12] A. Portevin, M. Bonnot, Compt. Rend. Acad. Sci. Paris, 196 (1933) 1603-1605 *(in French).*

[13] H. Witte, Z. Angew. Mineral., 1 (3) (1938) 255-268 *(in German).*

[14] H. Witte, Metallwirtschaft, 18 (22) (1939) 459-463 *(in German).*

[15] Y. Komura, T. Matsunaga, Mater. Res. Soc. Symp. Proc., 21 (1984) 325-328.

[16] T. Matsunaga, E. Koders, Y. Komura, Acta Crystallogr., Sect. C: Cryst. Struct. Commun., 40 (10) (1984) 1668-1670.

[17] T. Matsunaga, Y. Komura, J. Jpn. Inst. Met, 50 (7) (1986) 611-615 *(in Japanese).*

[18] T. Matsunaga, J. Sci. Hiroshima Univ., Ser. A: Phys. Chem., 51 (3) (1987) 247-275.

[19] H. Klee, H. Witte, Z. Phys. Chem., 202 (1954) 352-378 *(in German).*

[20] L.J. Aschan, Acta Polytech. Scand., 11 (285) (1960) 1-63.

[21] D. Farkas, C.E. Birchenall, Metall. Trans. A, 16 (3) (1985) 323-328.

[22] V. Ganesan, H. Ipser, J. Non-Cryst. Solids, 205-207 (1996) 711-715.

[23] H. Ipser, V. Ganesan, F. Sommer, in COST 507: Definition of thermochemical and thermophysical properties to provide a database for the development of new light alloys (I. Ansara, A.T. Dinsdale, M.H. Rand), Office for Official Publications of the European Communities, Luxembourg, 1997, p.58-61.

[24] G. Nagorsen, H. Witte, Z. Anorg. Allg. Chem., 271 (3-4) (1953) 144-149 *(in German).*

[25] H.E. Swanson, E. Tatge, Nat. Bur. Stand. (U.S.), Circ., 539 (1) (1953) 1-95.

[26] G.V. Raynor, W. Hume-Rothery, J. Inst. Met., 65 (1939) 477-485.

[27] M.E. Straumanis, E.Z. Aka, J. Appl. Phys., 23 (3) (1952) 330-334.

[28] A.G.H. Andersen, Trans. AIME, 137 (1940) 331-350.

[29] R.W. Olesinski, G.J. Abbaschian, in Phase Diagrams of Binary Copper Alloys (P.R. Subramanian, D.J. Chakrabarti, D.E. Laughlin), ASM International, Materials Park, OH, 1994, p. 398-405.

[30] F.R. Morral, A. Westgren, Ark. Kemi, Mineral. Geol., 11B (37) (1934) 1-6.

[31] F. Weitzer, K. Remschnig, J.C. Schuster, P. Rogl, J. Mater. Res., 5 (10) (1990) 2152-2159.

[32] J.K. Solberg, Acta Crystallogr., Sect. A: Found. Crystallogr., 34 (5) (1978) 684-698.

[33] Y.I. Dutchak, Y.P. Yarmolyuk, Y.I. Fedyshin, Inorg. Mater., 11 (1975) 1047-1049.

[34] F. Gingl, P. Selvam, K. Yvon, Acta Crystallogr., Sect. B: Struct. Sci., 49 (2) (1993) 201-203.

[35] K.H. Lieser, H. Witte, Z. Metallkd., 43 (1952) 396-401 (*in German*).

[36] T. Jantzen, S.G. Fries, I. Hurtado, M.H.G. Jacobs, P.J. Spencer, in COST 507: Definition of thermochemical and thermophysical properties to provide a database for the development of new light alloys, Office for Official Publications of the European Communities (I. Ansara, A.T. Dinsdale, M.H. Rand), Luxembourg, 1997, p.73-82.

[37] C. He, Y. Du, H. Chen, H. Ouyang, Int. J. Mater. Res., 99 (8) (2008) 907-911.

[38] A.T. Dinsdale, Calphad, 15 (4) (1991) 317-425.

[39] C.A. Coughnanowr, I. Ansara, R. Luoma, M. Hamalainen, H.L. Lukas, Z. Metallkd., 82 (7) (1991) 574-581.

[40] X. Yan, Y.A. Chang, J. Alloys Compd., 308 (1-2) (2000) 221-229.

[41] D. Kevorkov, R. Schmid-Fetzer, F. Zhang, J. Phase Equilib. Diff., 25 (2) (2004) 140-151.)

[42] O. Redlich, A.T. Kister, Ind. Eng. Chem., 40 (2) (1948) 345-348.

[43] W. Xiong, Y. Du, W. Zhang, W. Sun, X. Lu, F. Pan, Calphad, 32 (4) (2008) 675-685.

[44] B. Sundman, B. Jansson, J. Andersson, Calphad, 9 (2) (1985) 153-190.

[45] Y. Du, R. Schmid-Fetzer, H. Ohtani, Z. Metallkde., 88 (7) (1997) 545-556.